Journal of Experimental Botany, Vol. 58, No. 4, pp. 827–838, 2007
Imaging Stress Responses in Plants Special Issue
doi:10.1093/jxb/erl115 Advance Access publication 12 September, 2006

Journal of Experimental Botany

SPECIAL ISSUE PAPER

Use of thermal and visible imagery for estimating crop water status of irrigated grapevine*

M. Möller[1,†], V. Alchanatis[2], Y. Cohen[2], M. Meron[3], J. Tsipris[3], A. Naor[4], V. Ostrovsky[2], M. Sprintsin[5] and S. Cohen[1]

[1] *Institute of Soil, Water and Environmental Sciences, Agricultural Research Organization (ARO), The Volcani Center, PO Box 6, 50250 Bet Dagan, Israel*

[2] *Institute of Agricultural Engineering, Agricultural Research Organization (ARO), The Volcani Center, PO Box 6, 50250 Bet Dagan, Israel*

[3] *Crop Ecology Laboratory, Migal, PO Box 831, 11016 Kiryat Shmona, Israel*

[4] *Golan Research Institute PO Box 97, 12900 Katzrin, Israel*

[5] *The J Blaustein Institute for Desert Research, Ben-Gurion University of the Negev, Sede-Boker Campus 84990, Israel*

Received 1 May 2006; Accepted 5 July 2006

Abstract

Achieving high quality wine grapes depends on the ability to maintain mild to moderate levels of water stress in the crop during the growing season. This study investigates the use of thermal imaging for monitoring water stress. Experiments were conducted on a wine-grape (*Vitis vinifera* cv. Merlot) vineyard in northern Israel. Irrigation treatments included mild, moderate, and severe stress. Thermal and visible (RGB) images of the crop were taken on four days at midday with a FLIR thermal imaging system and a digital camera, respectively, both mounted on a truck-crane 15 m above the canopy. Aluminium crosses were used to match visible and thermal images in post-processing and an artificial wet surface was used to estimate the reference wet temperature (T_{wet}). Monitored crop parameters included stem water potential (Ψ_{stem}), leaf conductance (g_L), and leaf area index (*LAI*). Meteorological parameters were measured at 2 m height. *CWSI* was highly correlated with g_L and moderately correlated with Ψ_{stem}. The *CWSI*-g_L relationship was very stable throughout the season, but for that of *CWSI*-Ψ_{stem} both intercept and slope varied considerably. The latter presumably reflects the non-direct nature of the physiological relationship between *CWSI* and Ψ_{stem}. The highest R^2 for the *CWSI* to g_L relationship, 0.91 (n=12), was obtained when *CWSI* was computed using temperatures from the centre of the canopy, T_{wet} from the artificial wet surface, and reference dry temperature from air temperature plus 5 °C. Using T_{wet} calculated from the inverted Penman–Monteith equation and estimated from an artificially wetted part of the canopy also yielded crop water-stress estimates highly correlated with g_L (R^2=0.89 and 0.82, respectively), while a crop water-stress index using 'theoretical' reference temperatures computed from climate data showed significant deviations in the late season. Parameter variability and robustness of the different *CWSI* estimates are discussed. Future research should aim at developing thermal imaging into an irrigation scheduling tool applicable to different crops.

Key words: Canopy temperature, CWSI, energy balance, infrared thermography, irrigation scheduling, stem water potential, stomatal conductance, *Vitis vinifera*.

Introduction

Water is a major factor affecting both quality and quantity of wine grapes (*Vitis vinifera* L.). Excessive water leads to increased vegetative growth and yield, but grape quality

* Contribution No. 610/06 from the Agricultural Research Organization, The Volcani Center, Bet Dagan, Israel.
† To whom correspondence should be addressed. E-mail: marmoeller@yahoo.de

parameters, such as sugar content, pigment formation, acidity, and wood maturation of the wine are negatively affected (Van Leeuwen and Seguin, 1994; Schultz and Gruber, 2005). Severe water stress on the other hand will induce stomatal closure (Escalona *et al*., 1999), causing strongly reduced or no assimilative activity and shoot growth and negative effects on wood maturation and sugar content. Maintaining a slight-to-moderate water deficit and thus inducing a certain level of stress can be very beneficial in grapevine cultivation as it stimulates optimal quality parameters without significantly compromising yield. In order to achieve this, crop water status must be measured accurately and reliably with the aim of maintaining a predetermined level of mild stress. Crop water status is preferably estimated by the direct sensing of plant water-stress parameters, like stem water potential and leaf conductance, rather than soil-based measurement approaches, which are prone to cumulative errors, require many sensors and may not be representative due to soil heterogeneity (Jones, 1990, 2004; Schultz and Gruber, 2005). For most crops, with the possible exception of anisohydric species whose leaf water potential decreases at increased water stress (Tardieu and Simonneau, 1998), for example, cotton and sunflower, leaf conductance is very sensitive to actual crop water stress, and therefore may give a better indication of stress than tissue-based measures such as leaf and stem water potential (Jones, 2004). However, leaf conductance is sensitive to other factors, the spatial coverage of spot leaf conductance measurements made with porometers is very limited and leaf-to-leaf variations require much replication for reliable data, so porometry is unsuitable for commercial applications (Hsiao, 1990). As a consequence, despite its accuracy the application of porometry as a measure for crop water status has been limited to research studies.

From energy balance considerations, it can be shown that leaf temperature is inversely correlated with transpiration rate and stomatal conductance (Fuchs and Tanner, 1966; Fuchs, 1990; Jones, 1992). The usefulness of canopy temperature as a measure of 'crop water stress' was recognized in the 1960s (Tanner, 1963; Gates, 1964). The 'Crop Water Stress Index', *CWSI* (Idso *et al*., 1981; Jackson *et al*., 1981; Idso, 1982; Jackson, 1982), is based on the difference between canopy temperature, as measured by infrared thermometry (IRT), and that of a 'non water-stressed baseline' referring to the temperature of a well-watered crop. Despite robust results with the *CWSI* approach from arid and semi-arid regions, limitations of its use as a routine tool stem from its high sensitivity to climate factors such as radiation and wind speed (Jackson *et al*., 1988; Jones, 1999*a*), which are not included in the computation of *CWSI*, and from the need to establish crop-specific non-water-stressed baselines for different agroclimatic zones.

In order to overcome these difficulties, a normalized *CWSI* using natural wet and dry reference surfaces (T_{wet} and T_{dry}, respectively), for example, wetted or fully transpiring section of the canopy, was proposed by Clawson *et al*. (1989). This approach was used by Jones *et al*. (1999*b*), and the successful use of wet and dry reference plants has been reported by Leinonen and Jones (2004). However, these natural surfaces might not necessarily be uniform and difficulties are likely to arise with regard to their reproducibility. Meron *et al*. (2003) addressed problems related to low uniformity and reproducibility by using a wet artificial reference surface (WARS) for estimating T_{wet} and by taking the upper base line temperature, T_{dry}, as T_{air}+5 °C, based on earlier publications (Irmak *et al*., 2000). The successful use of these artificial references on a sub-plot scale has been reported by Cohen *et al*. (2005), who used thermal imagery for evaluating and mapping the leaf water potential of cotton under various irrigation regimes.

Another alternative measure of crop stress which can be derived from thermal imagery is the spatial variability of leaf temperature, which should be related to the spatial variability of g_L. Fuchs (1990) derived the variance of leaf temperature from a theoretical analysis of plant energy balance, and showed that it should be directly related to stress. Jones (1999*b*; Jones *et al*., 2002) suggested that this measure could be appropriate for crops with uniform full cover.

Much of the early work on thermography and *CWSI* estimation was based on handheld thermometers, which measure a temperature average over a single target area. Soil, trunk or dead tissue might be included in the sample area, potentially leading to considerable errors in estimated canopy temperature, particularly in sparse vegetation (Moran *et al*., 1994; Inoue *et al*., 1994). Recent technological advances in thermal imagery offer the potential to acquire spatial information on surface temperature in high resolution. Thermal, in conjunction with visible and near infrared (NIR) images enable the exclusion of non-leaf material in the estimate of canopy temperature and the possibility of selecting specific parts of the canopy for water-stress estimation (Jones *et al*., 2004).

Despite these recent significant improvements in the hard- and software used in thermal imaging, there is a current lack of knowledge in linking remotely measured canopy temperature and *CWSI* to 'true' ground-based measures of crop water stress, such as leaf conductance and water potential in the leaf or stem. However, knowledge of these relationships is required in order to translate thermal imagery data accurately into water-stress estimates, which can then serve as irrigation decision support tools.

In the present study, the potential of using thermal and visible images for the in-field estimation of crop water status of grapevine under three different irrigation regimes was investigated. The specific aims were (i) to compare thermal based *CWSI* estimates with plant water status parameters, (ii) to test the performance of different reference surfaces for *CWSI* computation, and (iii) to

develop models for estimating stem water potential and stomatal conductance based on thermal and visible images.

Materials and methods

Field plots

The field experiments were carried out at Kibbutz Yiftah, Israel (33° 10′ N; 35° 55′ E; 475 masl) during the summer of 2005. Times refer to Israel daylight saving time. Measurements were made on grapevines (*Vitis vinifera* cv. Merlot) planted in 1996 in a N–S direction with a vine and row spacing of 1.5 m and 3.0 m, respectively. Crop height varied between 2.0 m and 2.5 m. Soil texture was 50% clay, 24% silt, and 26% sand, with a pH of 7.4, a lime content of 9.5% and an EC (saturated paste) of 0.8 dS m^{-1}. Vines were irrigated using a drip system with one line per row (integral drippers, emitter spacing 0.5 m, flow rate 2.3 l h^{-1}, pressure compensated, Netafim, Israel). Three different treatments were applied: mild water stress (I), moderate water stress (II), and severe water stress (III). In order to maintain these treatments along the season, stem water potential (Ψ_{stem}) was measured once or twice a week and irrigation was applied when this reached the following thresholds: −9.5 bar (I), −12.0 bar (II), and −14.0 bar (III). Both timing and amount of water applications were adjusted for each treatment individually on a trial and error basis in order to maintain stem water potential near these thresholds. Commencement of irrigation and total amount of applied water until harvest were as follows: 24 May, 454 mm (I), 1 July, 150 mm (II); and 26 July, 23 mm (III), which was 89%, 29%, and 5%, respectively, of seasonal crop water requirements (509 mm) of fully watered grapevines, computed after Allen *et al*. (1998) using a crop coefficient equal to 0.3, 0.7, and 0.45 in the initial, mid-season and late-season development stages, respectively. There were three parallel experimental rows of which the two outer rows served as guard rows while measurements were conducted in the central row. In all three rows, three replicates per treatment, each consisting of seven vines, were laid out randomly in three main blocks.

Image acquisition and processing

Acquisition of thermal and colour images: Thermal images of the plots were taken with an uncooled infrared thermal camera between 11.30 h and 15.00 h on 23 June, 12 July, 25 July, and 9 August 2005. The camera (ThermaCAM model SC2000, FLIR systems) had a 320×240 pixel microbolometer sensor, sensitive in the spectral range of 7.5–13 μm, and a lens with an angular field of view of 24°. Digital colour images were acquired with a digital camera (DSC-F717, Sony Inc.) that was attached to the thermal camera. The two cameras were mounted on a truck-crane about 15 m above the canopy. The canopy height was about 2 m, so that the linear field of view at the canopy level was 2×(15–2)×tan(24°/2)=5.5 m (i.e. 1.7 cm $pixel^{-1}$). This resolution enabled differences between leaves and soil, as well as the selection of pixels that contained sunlit leaves, to be distinguished. Aluminium crosses were placed in the camera's field of view in order to geo-reference the digital RGB and the thermal images (Fig. 1). A wet artificial reference surface (WARS) was also placed in the camera's field of view (Fig. 1). The WARS was constructed as follows (Meron *et al*., 2003). A 5 cm thick slab of expanded polystyrene foam was floated in a 40 cm×30 cm×12 cm plastic tray, covering most of the water surface. It was coated with a doubled piece of 0.5 mm thick water absorbent non woven polyester and viscose mixture cloth (Spuntech, Israel), overlaid on another 2 mm thick polyester non-woven water-absorbent cloth. The edges of the clothes served as a wick, soaking up water to replace evaporation, and the polystyrene foam insulated the float from the background. This floating set-up provided horizontal and vertical alignment and a permanently wet surface of reproducible radiometric and physical properties. The outer layer sensed by the IR image is thus insulated from the water bath and essentially an independent ~2 mm thick white water layer.

Processing of thermal images: Thermal images were processed with digital image processing tools. The raw thermal images were obtained in the FLIR Systems' proprietary format and converted to grey-scale images as described by Cohen *et al*. (2005). The centres of the aluminium crosses were selected as geographical control points (GCPs) and the thermal and colour digital images were aligned and registered using Matlab R13 software (Mathworks Inc.). The colour image was used to select canopy pixels with specific features, such as sunlit pixels. This was performed by transforming the colour image from the RGB to the Hue-Saturation-Intensity (HSI) colour space and then by applying threshold values in each of the colour components. The above procedure yielded to a binary image where pixels belonging to the selected canopy fraction are represented by logical 'one' and all other pixels are represented by logical 'zero'. The HSI threshold values were determined interactively by an operator while visually inspecting the resulting image. Once a set of threshold values was chosen, the consequent images were processed using the same set of threshold values. Using the above procedure two types of masks were created: masks of soil and masks of both soil and shadowed leaves (Fig. 2). A proprietary software was developed by our research group that implemented the above process, constructed the masks, and then used only pixels with a corresponding mask of logical 'one' in the statistical analysis of the temperature in the thermal images.

Meteorological and physiological measurements

Global radiation, wind speed, air temperature, and relative humidity were measured 2 m above-ground by a meteorological station

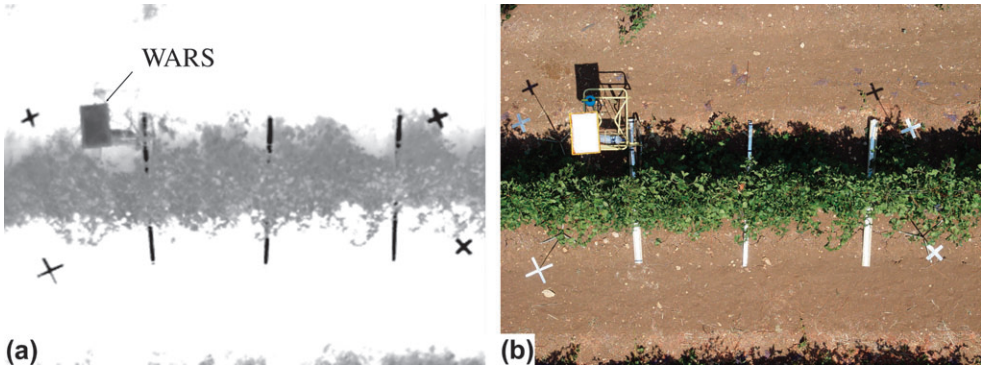

Fig. 1. Thermal (a) and colour (b) images of vines.

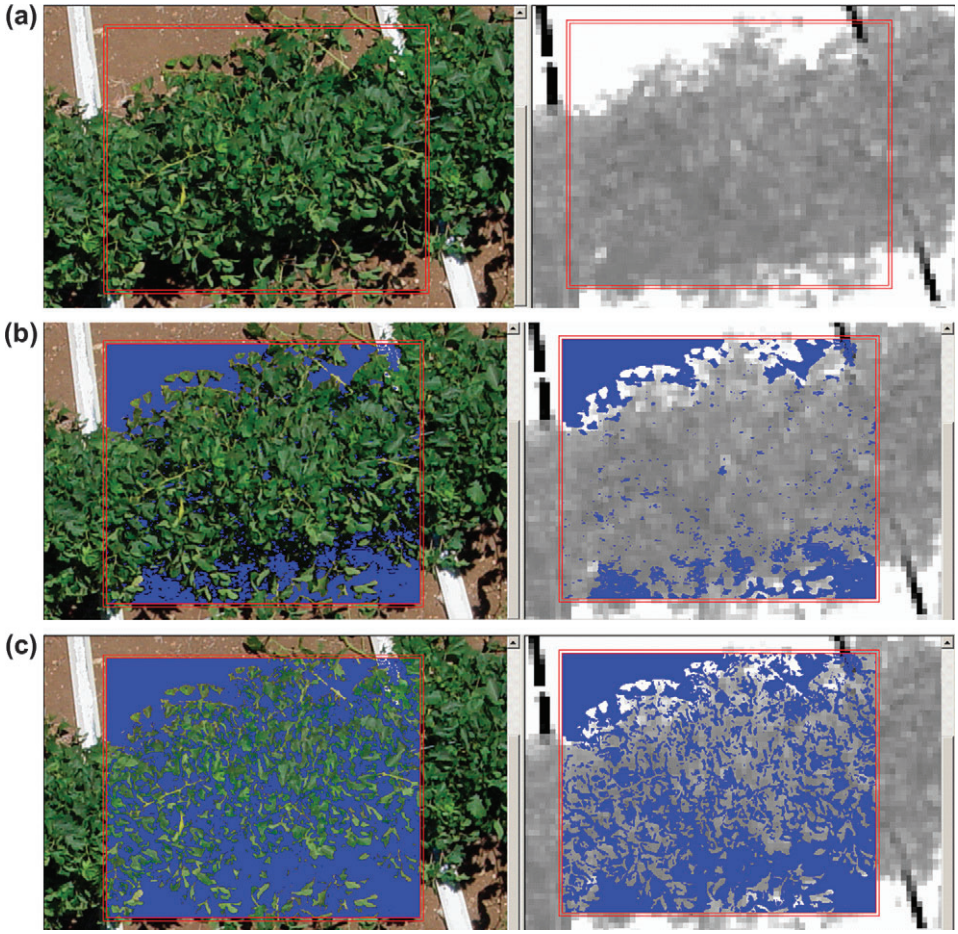

Fig. 2. Fusion of thermal and colour images for extraction of different canopy fractions. (a) Original colour and TIR images, (b) soil mask, (c) mask of both soil and shadowed leaves.

positioned within the experimental plot. The sampling rate was 0.1 Hz and 1 min averages were logged to a data acquisition system (CR10X, Campbell Sci., Logan, Utah). In addition, hourly climate data and 24 h Penman–Monteith reference evapotranspiration are available from the Kadesh meteorological station, located less than 1 km from the experimental site.

Once or twice weekly, stem water potential Ψ_{stem} was determined as follows: six shaded leaves per treatment in the lower part of the canopy were covered with aluminium foil-coated plastic bags at around 11.00 h for at least 90 min, in order to allow Ψ_{stem} and leaf water potential to equilibrate (Naor, 1998). After this equilibration period, the leaves were removed and covered with a plastic bag and Ψ_{stem} was measured using a pressure chamber (ARIMAD, Kfar Haruv, Israel), following the same procedure as outlined by Meron *et al*. (1987) for leaf water potential measurements in cotton.

Leaf area index *LAI* was estimated by Gap Fraction Inversion (Cohen *et al*., 1997, 2000) on 19 July and 8 August. Measurements were done at three different zenith angles on three vines per treatment using a linear photosensor array probe (model Sunlink, Decagon Inc., Pullman, WA).

On days on which thermal and RGB images were taken, plant physiological measurements were carried out as follows: immediately following thermal and RGB image acquisition in each treatment plot, stomatal conductance and stem water potential were measured in the two vines in the centre of the respective plot. Ψ_{stem} was measured with four replications per treatment plot on 23 June and 25 July, and two replications on 12 July and 9 August, respectively. Stomatal conductance was measured in sun-exposed fully developed leaves in the upper part of the canopy using a steady-state porometer (Li-Cor model 1600, Lincoln, Nebraska, USA). There were 10 replications per treatment plot on 12 and 25 July and 15 and 20 replications on 9 August and 23 June 2005, respectively.

Theory and equations

Crop water stress index *CWSI* was calculated after Jones (1992) as:

$$CWSI = \frac{T_{canopy} - T_{wet}}{T_{dry} - T_{wet}} \quad (1)$$

where T_{canopy} is actual canopy temperature obtained from the thermal image and T_{wet} and T_{dry} are the lower and upper boundary temperatures representing a fully transpiring leaf with open stomata and a non-transpiring leaf with closed stomata, respectively. Note that T_{wet} and T_{dry} are equivalent to T_{base} and T_{max} in the original formulation of *CWSI* by Idso *et al*. (1981). For an estimation of T_{canopy}, different sections of the canopy were tested: all canopy, sunlit canopy, centre of the canopy, and sunlit leaves at the centre of the canopy. T_{wet} was taken as the average temperature of the wet artificial reference surface (WARS). Two additional alternative estimates for T_{wet} were tested: (i) spraying part of the canopy with water some 20 s

prior to thermal image acquisition (referred to as $CWSI_{wet\_canopy}$) and (ii) as derived from the energy balance as (Jones, 1999*a*; referred to here as $CWSI_{T\_wet}$):

$$T_{wet} = T_a + \frac{r_{HR} r_{aW} \gamma R_{ni}}{\rho_a c_p [\gamma (r_{aW}) + \Delta r_{HR}]} - \frac{r_{HR} VPD}{\gamma r_{aW} + \Delta r_{HR}} \quad (2)$$

where T_a is air temperature, r_{HR} is the resistance to heat and radiative transfer (Jones, 1992, 1999*a*) using a characteristic leaf dimension of 0.1 m, r_{aW} is the boundary layer resistance for water vapour (Jones, 1992), γ is the psychrometric constant, R_{ni} is net radiation, ρ_a is the density of air, c_p is the specific heat of air, and Δ is the slope of the saturation vapour-pressure curve.

T_{dry} was estimated by adding 5 °C to the measured dry bulb temperature, as suggested by Irmak *et al*. (2000) and used by Cohen *et al*. (2005). As a second estimate for T_{dry}, the concept of isothermal radiation was used (Jones, 1999*a*):

$$T_{dry} = T_a + \frac{r_{HR} R_{ni}}{\rho_a c_p} \quad (3)$$

CWSI that uses equations 2 and 3 for determining T_{wet} and T_{dry} is referred to as I_2.

Soil water deficit SWD_i on day i was calculated from irrigation records I_{net} and estimated crop water use ET_c:

$$SWD_i = SWD_{i-1} + ET_{c,i} - I_{net,i} \quad (4)$$

assuming that *SWD* at the end of the rainy season (30 April) was zero and that no runoff, rainfall, deep percolation, and capillary rise occurred during the calculation period. ET_c was estimated from reference evapotranspiration, the crop coefficient curve K_c for grapevines (initially 0.30, mid-season 0.70, and end of season 0.45; Allen *et al*., 1998) and a dimensionless transpiration reduction factor K_s estimated from Allen *et al*. (1998):

$$K_{S,i} = \frac{1000(\theta_{FC} - \theta_{WP}) D_{rz} - SWD_{i-1}}{(1-p)[1000(\theta_{FC} - \theta_{WP}) D_{rz}]} \quad (5)$$

where soil water content at field capacity θ_{FC} and permanent wilting point θ_{WP} at the site are estimated as 0.48 and 0.32, respectively (Achtnich, 1980), the rooting depth D_{rz} is 1.5 m and p is the maximum allowable depletion of total available soil water that does not cause a reduction in evapotranspiration (=0.45 for grapevine; Allen *et al*., 1998).

Results

Climate parameters and direct measurements of crop water status

An overview of the meteorological conditions prevailing during the period of thermal imaging and *CWSI* computation is given in Fig. 3, and the deviation of daily climate parameters on the four thermal imaging days from the seasonal average is presented in Table 1. Radiation measurements indicate clear sky conditions on all four days, except for the period from 11.25 h to 12.25 h on 25 July (Fig. 3a), when clouds modulated solar radiation. Temperatures were above the seasonal average on all four days, and 12 July was one of the hottest and driest days of the summer. During the period of the day when crop water stress measurements were made, both air temperature and vapour pressure deficit were relatively constant on 12 July

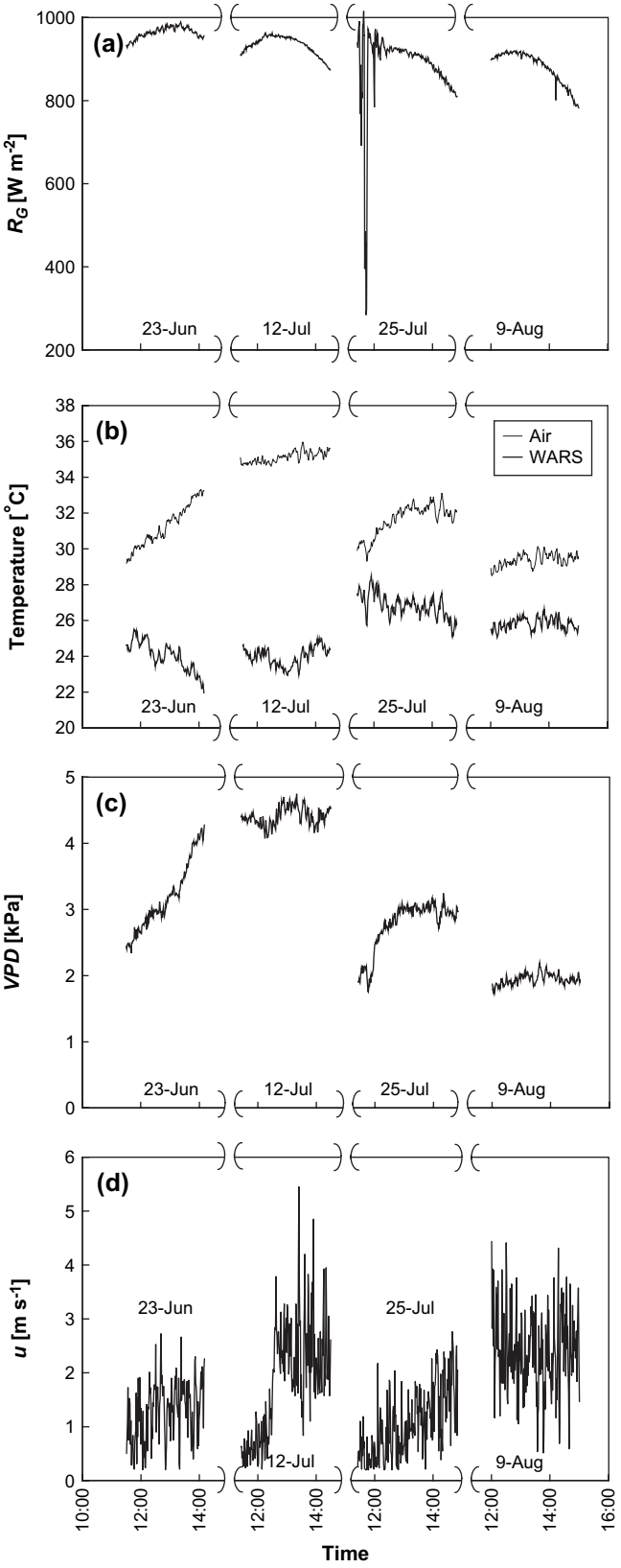

Fig. 3. Variation in global radiation R_G (a), air temperature and temperature of the wet artificial reference surface–WARS (b), vapour pressure deficit *VPD* (c), and wind speed *u* (d) during thermal imaging on 23 June, 12 and 23 July, and 9 August 2005.

and 9 August. By contrast, a steady 4 °C increase in air temperature was recorded on 23 June between 11.30 h and 14.10 h and a 3.5 K rise occurred on 25 July between 11.45 h and 14.20 h. Temperature increases on both days coincided with increases in vapour pressure deficit (*VPD*), which was particularly marked on 23 July, rising by 1.9 kPa from 11.35 h to 14.10 h. Wind speeds prevailing on these two days (23 June and 25 July) were relatively low, and increased slightly during the 4 h of thermal imaging. Daily wind speeds on 12 July and 9 August were higher than the seasonal average (Table 1), remaining relatively constant during the 4 h of measurements on 9 August, but rising sharply on 12 July at around 12.30 h, which indicates the onset of the Mediterranean sea-breeze on that day. These data represent a relatively wide range of climatic conditions for Israel's predominantly clear-sky summer.

The seasonal course of measured midday stem water potential is shown in Fig. 4. Ψ_{stem} was significantly higher (*t* test, P=0.05) in treatment I (crosses) than in the other two treatments (open triangles and filled circles) starting on 20 June, some 27 d after commencement of irrigation in this treatment. Water applications in treatment II started on 1 July and Ψ_{stem} was significantly higher than in treatment III immediately thereafter, except for 11 July. The seasonal minimum of Ψ_{stem} was −9.5, −11.8, and −16.5 bar in treatments I, II, and III, respectively.

Table 1. *Seasonal mean of climate parameters at Kadesh meteorological station (1 May through 31 August) and deviation from mean on the four days of thermal imaging*

	Mean	23 June	12 July	25 July	9 August
R_G (MJ m^{-2} d^{-1})	27.2	+8.4%	+8.4%	−1.7%	−2.9%
T_{mean} (°C)	23.8	+0.7 K	+4.2 K	+1.8 K	+1.6 K
u_{2m} (m s^{-1})	1.8	+10.9%	+45.1%	−30.6%	+61.1%
VPD (kPa)	1.76	+10.3%	+57.9%	−1.9%	−26.7%

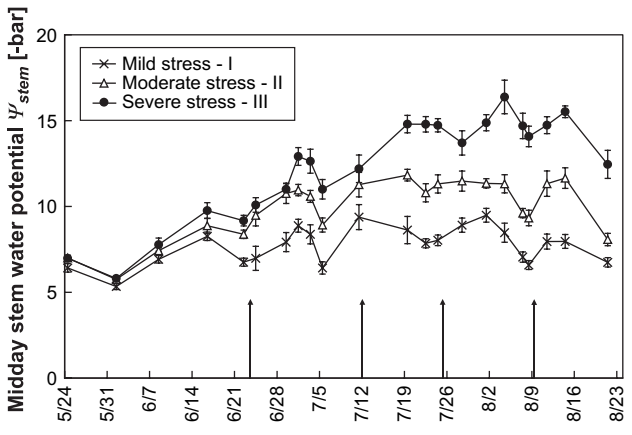

Fig. 4. Seasonal course of midday stem water potential measured in the three water-stress treatments. Vertical bars represent two standard errors of the mean. Vertical arrows indicate the days when thermal and visible images were acquired.

Average g_L and Ψ_{stem} measured during thermal and colour image acquisition are summarized in Table 2. The effects of the stress treatments on Ψ_{stem} and g_L were highly significant on all four dates (ANOVA). However, differences in g_L and Ψ_{stem} between treatments II and III were only significant on the 2nd and 3rd thermal imaging days, respectively. A strong positive correlation found between Ψ_{stem} and g_L (R=0.84; significant at P <0.01) on a seasonal basis was even higher when individual days were considered (Table 3). The slope of the regression curve decreased over the 4 d of measurement, indicating that for a given stomatal conductance, a lower stem water potential was observed as time progressed. This fact is corroborated by daily average values of Ψ_{stem} and g_L in treatments II and III (Table 2). It is noted that the intercept of the empirical Ψ_{stem}–g_L relationships was nearly constant, but significantly lower on the last day of measurement (Table 3). A relatively low correlation coefficient was found on 12 July. This was accompanied by a relatively large standard error of some Ψ_{stem} data points. The number of replicates per block on that date was two leaves as compared to four leaves on 23 June and 25 July, the range of Ψ_{stem} values was small, and differences between treatments II and III were not significant (see also Table 2a). Therefore, it is presumed that the low correlation coefficient is due to inaccuracies in Ψ_{stem} measurement.

Leaf area index

Treatment I (mild water stress) had the highest *LAI* on both days of measurement (Table 4; 19 July and 8 August), but differences between treatments II and III were not significant. In the severe water stress treatment III, *LAI* did not change significantly during the 20 d between measurements while total irrigation was 10 mm. *LAI* in treatments I and II increased by approximately 0.2, while irrigation was 117 and 71 mm, respectively. These results confirm that the irrigation regimes produced three long-term levels of crop water status.

Relationships between CWSI *and measured crop water status*

For estimation of T_{canopy}, different sections of the canopy were used: all canopy, sunlit canopy, centre of the canopy, and sunlit leaves from the centre of the canopy. The centre of the canopy yielded the best results (i.e. highest correlation coefficients for the relationship between *CWSI* and g_L) and there was no significant difference in correlation coefficients obtained from the centre of the canopy or its sunlit fraction. Therefore, in the results presented hereafter *CWSI* was based on temperature of the centre of the canopy.

Relationships between *CWSI* and stem water potential and between *CWSI* and leaf conductance are shown for individual days in Figs 5 and 6. High correlations were

Table 2. *Average stem water potential (a) and leaf conductance (b) per treatment measured on the four days of thermal imaging*

Levels of significance are from ANOVA. Values in the same column with the same letter are not significantly different at P=0.05, according to Tukey-Kramer HSD test (JMP, 2002).

(a) Treatment	23 June	12 July	25 July	9 August
	Ψ_{stem} (−bar)	Ψ_{stem} (−bar)	Ψ_{stem} (−bar)	Ψ_{stem} (−bar)
I: Mild water stress	6.8 a	8.3 a	7.4 a	6.5 a
II: Moderate water stress	9.4 b	11.3 b	10.8 b	10.2 b
III: Severe water stress	10.8 b	11.8 b	14.9 c	13.5 c
$P > F$	<0.01	<0.001	<0.001	<0.001
(b) Treatment	23 June	12 July	25 July	9 August
	g_L (mmol s^{-1} m^{-2})	g_L (mmol s^{-1} m^{-2})	g_L (mmol s^{-1} m^{-2})	g_L (mmol s^{-1} m^{-2})
I: Mild water stress	320 a	288 a	386 a	320 a
II: Moderate water stress	186 b	156 b	285 b	244 b
III: Severe water stress	132 b	85 c	109 c	134 c
$P > F$	<0.01	<0.001	<0.001	<0.001

Table 3. *Regression and statistical parameters from ANOVA for the relationship between stem water potential and leaf conductance on individual days*

	$g_L = a(-\Psi_{stem}) + b$						
	a	Significance	b	Significance	n	R^2	Significance
23 June	−47.2	P <0.0001	673.5	P <0.0001	9	0.95	P <0.0001
12 July	−44.7	P <0.001	633.3	P <0.0001	13	0.66	P <0.001
25 July	−34.2	P <0.0001	638.1	P <0.0001	18	0.93	P <0.0001
9 August	−25.5	P <0.0001	489.3	P <0.0001	18	0.86	P <0.0001

Table 4. *Comparison of leaf area index measured on 19 July and 8 August*

Levels of significance are from ANOVA. Values in the same column with the same letters are not significantly different at P=0.05, according to the Tukey-Kramer HSD test (JMP, 2002).

Treatment	*LAI*	
	19 July	8 August
I: Mild water stress	2.22 a	2.41 a
II: Moderate water stress	1.77 b	1.99 ab
III: Severe water stress	1.89 ab	1.90 b
$P > F$	<0.05	<0.05

found between g_L and Ψ_{stem} and *CWSI* using T_{dry} from air temperature +5 °C and T_{wet} from the wet artificial reference surface WARS. The slope of the *CWSI*–Ψ_{stem} relationship varied over time with steeper slopes observed later in the season. Lower coefficients of determination were observed on 12 July and 9 August when the number of replications per plot was lower. On the other hand, both slope and intercept of the *CWSI*-g_L relationship were found to be very stable over time (Fig. 6). A low coefficient of determination was found for the last day of measurement (9 August). It is noted that on that day leaf senescence, characteristic of the end of the growing season, was observed in some plots, and the hardy leaves selected for g_L may not have been representative of the whole canopy measured on the images. The seasonal *CWSI*-g_L relationship based on daily data per treatment is presented in Fig. 7. *CWSI* was highly correlated with measured stomatal conductance (R^2= 0.91, significant at P <0.0001).

Selection of different reference temperatures

The seasonal relationships between crop water stress indices based on different reference temperatures and measured stomatal conductance (Fig. 8) were all highly significant (P <0.01). When the last day of measurement (9 August) was not included in the analysis, the R^2 fit of the model generally increased. As mentioned earlier, on 9 August many leaves in all treatments had already started to lose pigments and become dry, and therefore leaf conductance of the whole canopy was probably lower than that of the leaves selected for measurement with the porometer. This reasoning is supported by the fact that all data points for 9 August lie to the right of the regression line (except for $CWSI_{wet\_canopy}$ in Fig. 8c), indicating that for a given

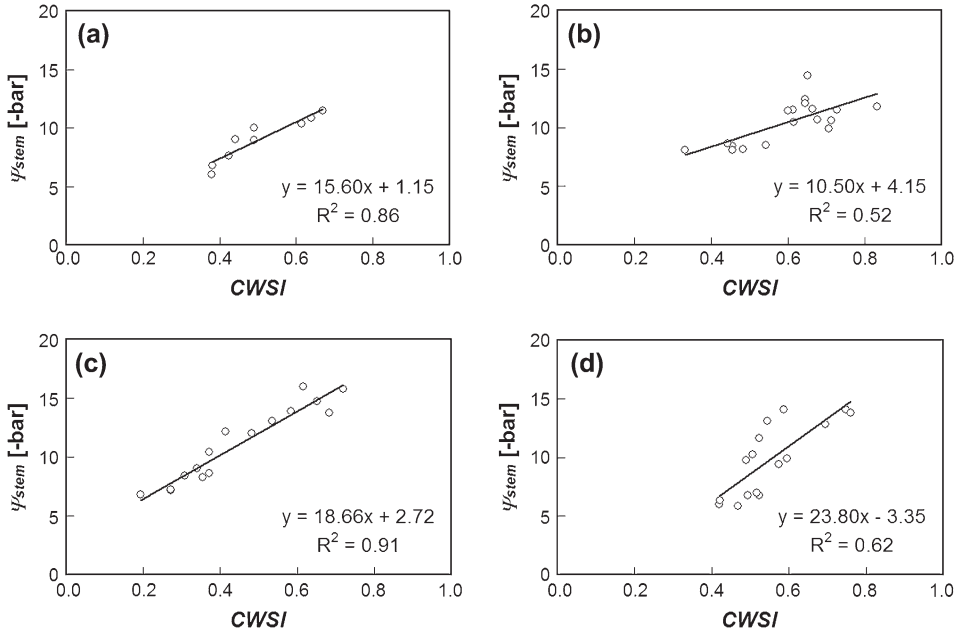

Fig. 5. Relationship between *CWSI* and Ψ_{stem} measured in individual plots on 23 June (a), 12 July (b), 25 July (c), and 9 August (d). ANOVA: n=9, R^2 significant at P <0.001 (a), n=18, P <0.001 (b), n=16, P <0.0001 (c), n=16, P <0.001 (d).

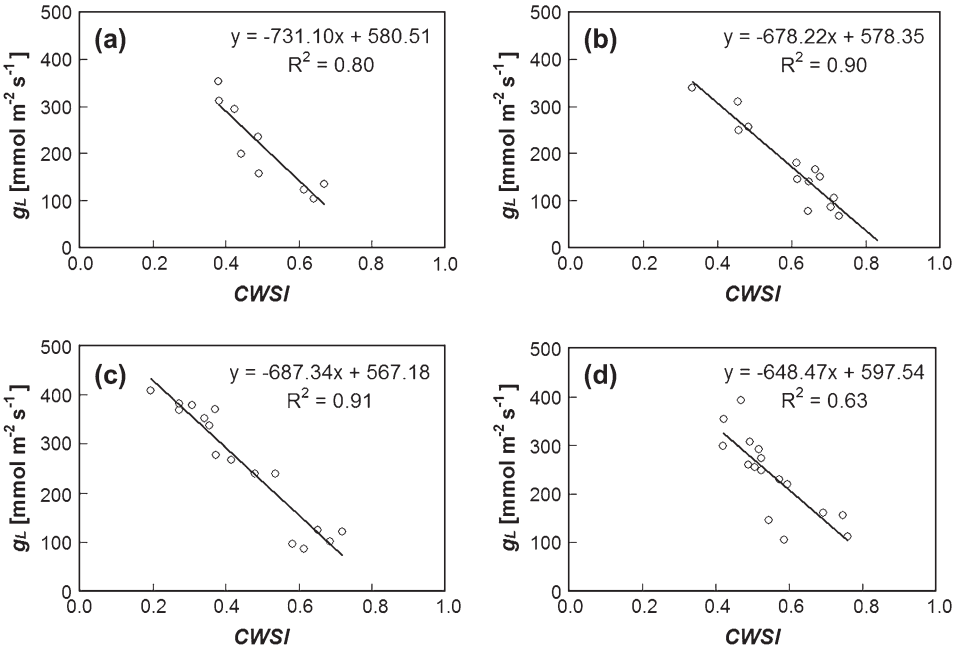

Fig. 6. Relationship between *CWSI* and g_L measured in individual plots on 23 June (a), 12 July (b), 25 July (c), and 9 August (d). ANOVA: n=9, R^2 significant at P <0.01 (a), n=14, P <0.0001 (b), n=16, P <0.0001 (c), n=16, P <0.001 (d).

measured leaf conductance, higher canopy temperature and hence water stress index was recorded on that day. Excluding these problematic data points had the least effect on the slope and intercept of the *CWSI*–g_L relationship (Fig. 8a) and a relatively small impact on the slope of the $CWSI_{T\_wet}$–g_L relationship (Fig. 8b) and the $CWSI_{wet\_canopy}$–g_L relationship (Fig. 8c). Slope, intercept and quality (R^2) of the relationship between the theoretical crop water stress index I_2 and g_L were significantly affected when the 9 August data were excluded but the $CWSI_{wet\_canopy}$ was least affected by the late season points, both in terms of regression line fit (R^2) and deviation of 9 August data from the other measurements. This is presumably due to the fact that unlike the other three indices, $CWSI_{wet\_canopy}$ refers to a reference

temperature extracted from the canopy image itself, thus incorporating seasonal effects on leaf colour and temperature. It can be shown mathematically that an equally increased wet reference temperature, induced by leaf colour changes, cancels out higher canopy temperatures, thus 'shifting' data points back to the left onto the regression line, as observed in the difference between Fig. 8d and c.

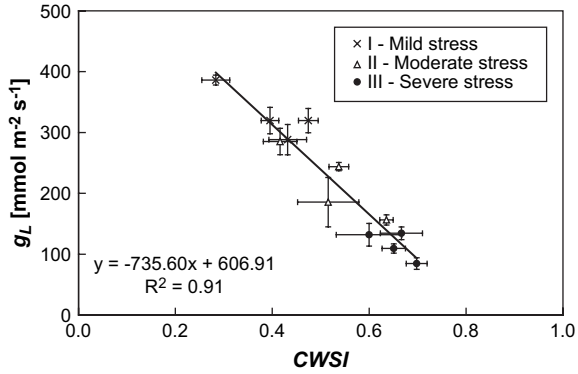

Fig. 7. Seasonal relationship between *CWSI* and measured g_L, treatment averages on individual days; n=12, R^2 significant at P <0.0001 (from ANOVA). Horizontal bars are two standard errors of mean *CWSI* and vertical bars represent two standard errors of the mean of g_L.

Discussion

Treatment and climate differentiation

It is important to base the relationships between remotely determined *CWSI* (from thermal imaging) and directly measured crop water stress on a broad range of climatic and crop physiological conditions. This improves the quality of the established relationship and provides insight as to whether the model is robust at various crop growth stages. In this context, the *CWSI*–Ψ_{stem} relationship proved inferior to *CWSI*–g_L (Figs 5, 7) because the former changed during the season. The difference between the two relationships highlights that physically *CWSI* is more closely related to g_L than to $\Psi_{stem.}$ The shift in the *CWSI*–Ψ_{stem} relationship may be from an adjustment in the plant response to water potential during the summer, which leads to higher leaf conductance for the same Ψ_{stem}; perhaps due to differences in osmotic adjustment in the irrigation treatments. This seasonally changing Ψ_{stem}–g_L relationship was also reported for peach (Marsal and Girona, 1997) and pear trees (Marsal *et al*., 2002). Midday Ψ_{stem} is commonly used for irrigation scheduling in commercial deciduous orchards in Israel (Naor, 2006), and was shown here to be highly correlated with *SWD* (Fig. 9), a parameter that is critical for irrigation management. Thus, the change in the *CWSI*–Ψ_{stem} relationship during the season might require

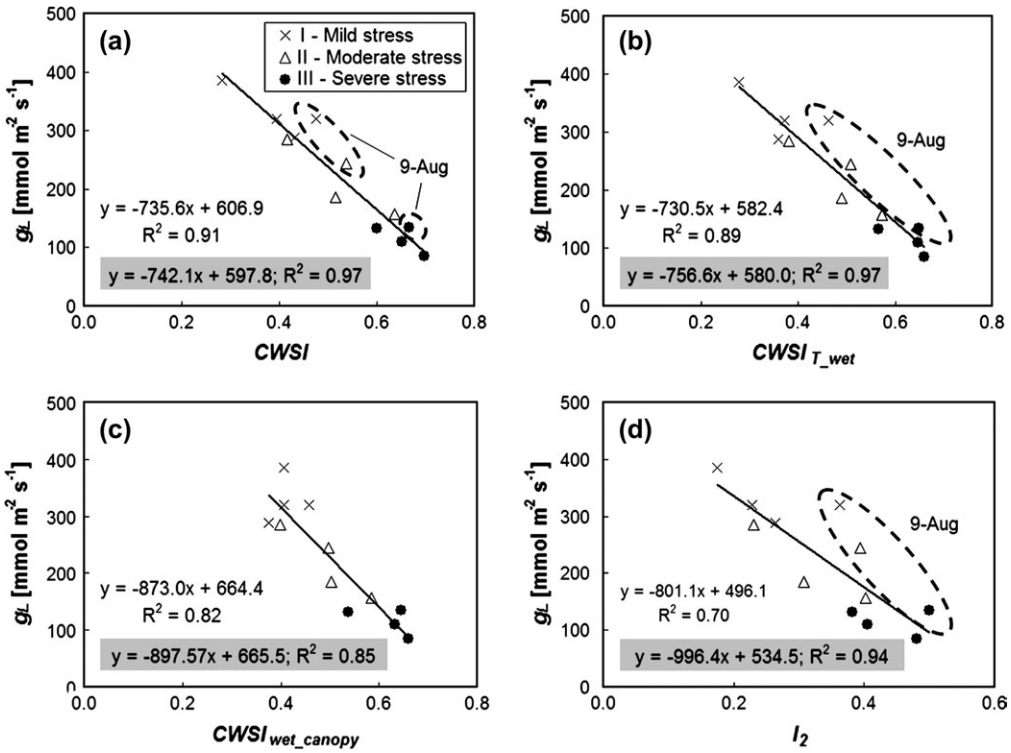

Fig. 8. Seasonal relationship between measured g_L and *CWSI* (a), $CWSI_{T\_wet}$ (b), $CWSI_{wet\_canopy}$ (c), and I_2 (d) for treatment averages on individual days. Linear regression functions (solid lines) are for all dates and regression equations and R^2 are for all dates (white background) and all dates except 9 August (grey background).

variable irrigation thresholds if *CWSI* is used for irrigation scheduling.

Full differentiation between the three water stress treatments occurred earlier in the season when leaf conductance is considered, as compared to stem water potential (Table 2). The influence of the irrigation treatments on the crop was also seen in *LAI* measured on two dates (Table 4). Measured Ψ_{stem} was thus less sensitive to the level of water stress than g_L during the first half of the growing season, although it should be noted that Ψ_{stem} estimation was based on a much smaller sampling size than were leaf conductance measurements.

Covering a wide range of climatic conditions during the experimental stage is desirable to (i) establish that the model is accurate and stable under all conditions and hence (ii) increase model reliability and accuracy when applied to other sites. Given the relatively uniform clear sky and hot Israeli summer climate, in this experiment a relatively wide range of climate conditions was covered, ranging from very hot, dry and windy conditions (12 July) to moderate temperatures, humid and windy conditions (9 August). The radiation regime was only representative of clear sky conditions. It is therefore believed that the conditions were representative of summer climate in clear-sky vine-growing regions of the temperate and subtropical zones.

Variability of canopy temperature and conductance

Fuchs (1990) suggested, based on a theoretical analysis, that variability of canopy temperature increases with crop stress and that this relationship might be used as an indicator of stress. Some variability in this study's results might result from inclusion of hot background soil in pixels at the edge of the canopy. In order to overcome this, threshold temperatures were defined and only the central part of the canopy was analysed. The standard deviation of canopy temperature in the thermal images ranged from 1.6 °C to 3.8 °C per treatment and day or 5–13% of the respective mean. However, the relationship between canopy temperature variability and water stress (measured as leaf conductance) was weak and statistically insignificant (R^2 <0.10; n.s.; data not shown). This agrees with conclusions drawn by Jones *et al*. (2002) that the Fuchs method (1990) might not be appropriate for row crops, such as grape vines, but rather might apply to homogeneous crops. However, an increased variability (expressed in the coefficient of variation) of stomatal conductance was observed at increased crop water stress (Fig. 10). It is not fully understood why this increased crop water stress was not reflected in increased variability of leaf temperature. Changes in leaf angle (away from the sun) and curling in stressed canopies might have prevented higher leaf temperatures, resulting in relatively uniform temperatures despite increased water stress and variability in leaf conductance.

Forecast quality and robustness of different CWSI *estimates*

Figure 8 demonstrates that *CWSI*, computed using T_{air}+5 °C and WARS for T_{dry} and T_{wet}, respectively, was the most precise crop water stress estimate. In addition to its accuracy, the use of an easily reproducible wet reference surface, and no climate data requirements other than air temperature, potentially make it an attractive stress detection tool for precision agriculture. When T_{dry} and T_{wet} were estimated from the inverted Penman–Monteith equation (equations 2, 3) solved with 1 min climate data (Fig. 8b, d) the R^2 was lower. The use of T_{wet_canopy} (Fig. 8c) as an estimate for T_{wet} should be considered for crop varieties with seasonably strongly variable reflectance and pigment content, since $CWSI_{wet\_canopy}$ proved to be the least affected by seasonal changes, although its overall accuracy was somewhat lower than that of *CWSI* (Fig. 8a). The quality of the seasonal *CWSI*–g_L relationships was

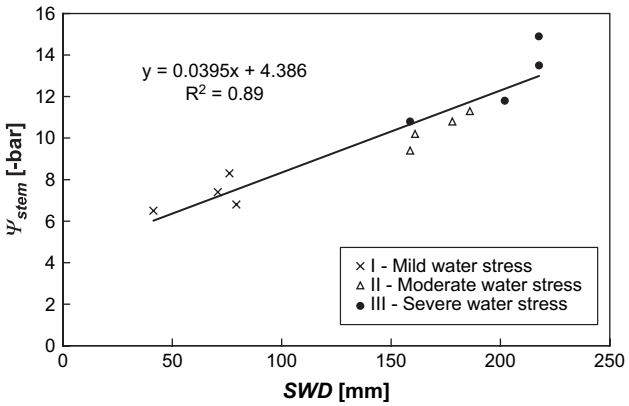

Fig. 9. Computed soil water deficit *SWD* versus measured stem water potential Ψ_{stem} on the four thermal imaging days, n=12, R^2 significant at P <0.0001.

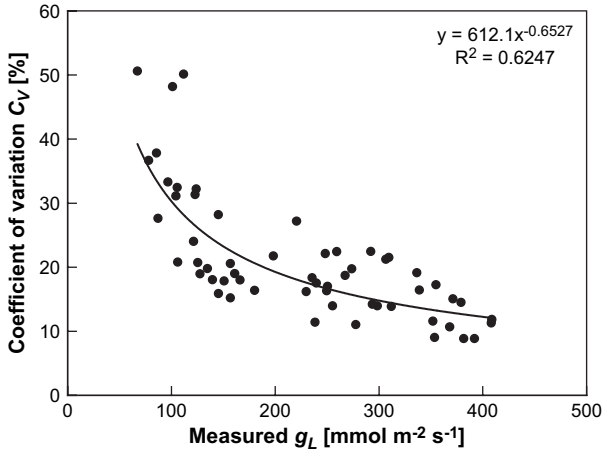

Fig. 10. Relationship between stomatal conductance and the coefficient of variation of stomatal conductance for plot averages on all four days, n=57, R^2 significant at P <0.0001.

presumably negatively affected by late season changes in pigment content. If the linear models from these relationships were used for irrigation scheduling, they might lead to over-irrigation in the late season.

It can be deduced from Fig. 8 that for a measured *CWSI*, the model underestimates 'true' leaf conductance on 9 August, and overestimates water stress. This late season discrepancy was particularly marked in the theoretical crop water stress index I_2, and might be of concern when applying *CWSI* for irrigation management in wine production where controlled stress is important for grape quality (Van Leeuwen and Seguin, 1994; Schultz and Gruber, 2005).

Conclusions

This study demonstrated that (i) fusion of thermal and visible imaging can improve the accuracy of remote *CWSI* determination and provide precise data on crop water status and stomatal conductance of grape vines; (ii) throughout the season *CWSI* computed with air temperature +5 °C and the artificial wet reference surface for T_{dry} and T_{wet}, respectively, was the most robust stress index; while (iii) stable linear relationships existed also when T_{wet} was derived from the energy balance ($CWSI_{T\_wet}$) and from image analysis of a wetted part of the canopy ($CWSI_{wet\_canopy}$).

Future studies should aim at (i) verifying and/or modifying the water stress models presented in this paper for other grape varieties and (ii) developing the $CWSI$–g_L relationships into a usable tool for irrigation management (i.e. timing and amount of water application) on a field scale.

Acknowledgements

This work was supported by grant No. TB-8006-04 from the Binational Agricultural Research and Development Fund and the Chief Scientist of the Israeli Ministry of Agriculture through project No. 458-0361-05.

References

Achtnich W. 1980. *Bewässerungslandbau.* Stuttgart: Eugen Ulmer Verlag, 126–146.

Allen RG, Pereira LS, Raes D, Smith M. 1998. *Crop evapotranspiration. Guidelines for computing crop water requirements.* Rome: FAO Irrigation and Drainage Paper 56.

Clawson KL, Jackson RD, Pinter PJ. 1989. Evaluating plant water stress with canopy temperature differences. *Agronomy Journal* **81,** 858–863.

Cohen S, Rao RS, Cohen Y. 1997. Canopy transmittance inversion using a line quantum probe for a row crop. *Agricultural and Forest Meteorology* **86,** 225–234.

Cohen S, Striem MJ, Bruner M, Klein I. 2000. Grapevine leaf area index evaluation by gap fraction inversion. *Acta Horticulturae* **537,** 87–92.

Cohen Y, Alchanatis V, Meron M, Saranga S, Tsipris J. 2005. Estimation of leaf water potential by thermal imagery and spatial analysis. *Journal of Experimental Botany* **56,** 1843–1852.

Escalona JM, Flexas J, Medrano H. 1999. Stomatal and non-stomatal limitations of photosynthesis under water stress in field-grown grapevines. *Australian Journal of Plant Physiology* **26,** 421–433.

Fuchs M. 1990. Infrared measurement of canopy temperature and detection of plant water stress. *Theoretical and Applied Climatology* **42,** 253–261.

Fuchs M, Tanner CB. 1966. Infrared thermometry of vegetation. *Agronomy Journal* **58**, 597–601.

Gates DM. 1964. Leaf temperature and transpiration. *Agronomy Journal* **56,** 273–277.

Hsiao TC. 1990. Measurements of plant water status. In: Stewart BA, Nielsen DR, eds. *Irrigation of agricultural crops.* Madison, WI: American Society of Agronomy Inc., 243–279.

Idso SB, Jackson RD, Pinter Jr PJ, Reginato RJ, Hatfield JL. 1981. Normalizing the stress-degree-day parameter for environmental variability. *Agricultural Meteorology* **24,** 45–55.

Idso SB. 1982. Non-water-stressed baselines: a key to measuring and interpreting plant water stress. *Agricultural Meteorology* **27,** 59–70.

Inoue Y, Sakuratani T, Shibayama M, Morinaga S. 1994. Remote and real-time sensing of canopy transpiration and conductance: comparison of remote and stem flow gauge methods in soybean canopies as affected by soil water status. *Japanese Journal of Crop Science* **63,** 664–670.

Irmak S, Haman DZ, Bastug R. 2000. Determination of crop water stress index for irrigation timing and yield estimation of corn. *Agronomy Journal* **92,** 1221–1227.

Jackson RD. 1982. Canopy temperature and crop water stress. *Advances in Irrigation Research* **1,** 43–85.

Jackson RD, Idso SB, Reginato RJ, Pinter Jr PJ. 1981. Canopy temperature as a drought stress indicator. *Water Resources Research* **17,** 1133–1138.

Jackson RD, Kustas WP, Choudhury BJ. 1988. A re-examination of the crop water stress index. *Irrigation Science* **9,** 309–317.

JMP. 2002. *Version 5.0.1.* Cary, NC: SAS Institute Inc., 1989–2002.

Jones HG. 1990. Plant water relations and implications for irrigation scheduling. *Acta Horticulturae* **278,** 67–76.

Jones HG. 1992. *Plants and microclimate*, 2nd edn. Cambridge: Cambridge University Press.

Jones HG. 1999*a.* Use of infrared thermometry for estimation of stomatal conductance as a possible aid to irrigation scheduling. *Agricultural and Forest Meteorology* **95,** 139–149.

Jones HG. 1999*b.* Use of thermography for quantitative studies of spatial and temporal variation of stomatal conductance over leaf surfaces. *Plant, Cell and Environment* **22,** 1043–1055.

Jones HG. 2004. Irrigation scheduling: advantages and pitfalls of plant-based methods. *Journal of Experimental Botany* **55,** 2427–2436.

Jones HG, Stoll M, Santos T, de Sousa C, Chaves MM, Grant OM. 2002. Use of infrared thermometry for monitoring stomatal closure in the field: application to grapevine. *Journal of Experimental Botany* **53,** 2240–2260.

Leinonen I, Jones HG. 2004. Combining thermal and visible imagery for estimating canopy temperature and identifying plant stress. *Journal of Experimental Botany* **55,** 1423–1431.

Marsal J, Girona J. 1997. Relationship between leaf water potential and gas exchange activity at different phonological stages and fruit load in peach trees. *Journal of the American Society for Horticultural Science* **3,** 415–421.

Marsal J, Mata M, Arbonés A, Rufat J, Girona J. 2002. Water stress limits for vegetative and reproductive growth of 'Bartlett' pears. *Acta Horticulturae* **596,** 659–664.

Meron M, Tsipris J, Charitt D. 1987. Pressure chamber procedures for leaf water potential measurements of cotton. *Irrigation Science* **8,** 215–222.

Meron M, Tsipris J, Charitt D. 2003. Remote mapping of crop water status to assess spatial variability of crop stress. In: Stafford J, Werner A, eds. *Precision agriculture.* Proceedings of the 4th European Conference on Precision Agriculture, Berlin, Germany. Wageningen: Academic Publishers, 405–410.

Moran MS, Clarke TR, Inoue Y, Vidal A. 1994. Estimating crop water deficit using the relation between surface-air temperature and spectral vegetation index. *Remote Sensing of Environment* **49,** 246–263.

Naor A. 1998. Relationships between leaf and stem water potentials and stomatal conductance in three field-grown woody species. *The Journal of Horticultural Science and Biotechnology* **73,** 431–436.

Naor A. 2006. Irrigation scheduling and evaluation of tree water status in deciduous orchards. *Horticulture Reviews* **32,** 111–165.

Schultz HR, Gruber BR. 2005. Bewässerung und 'Terroir'. Ergänzung oder Gegensatz? *Das Deutsche Weinmagazin* **1,** 24–28.

Tanner CB. 1963. Plant temperatures. *Agronomy Journal* **55,** 210–211.

Tardieu F, Simonneau T. 1998. Variability among species of stomatal control under fluctuating soil water status and evaporative demand: modeling isohydric and anisohydric behaviours. *Journal of Experimental Botany* **49,** 419–432.

Van Leeuwen C, Seguin G. 1994. Incidences de l'alimentation en eau de la vigne, appreciée par l'etat hydrique du feuillage, sur le développement de l'appareil végétatif et la maturation du raisin (*Vitis vinifera* variété Cabernet franc, Saint-Emilion 1990). *Journal International Sciences de la Vigne et du Vin* **28,** 81–110.